EVIDENCE FOR THE SEDIMENTARY ORIGIN OF IMBRIUM SCULPTURE AND LUNAR BASIN RADIAL TEXTURE

JAMES W. HEAD
Department of Geological Sciences, Brown University, Providence, R.I., U.S.A.

(Received 8 April, 1976)

Abstract. The Imbrium sculpture texture, a distinctive ridged and furrowed pattern radial to the Imbrium basin and seen in other basins, has long been debated as to its origin (internal, formed by basin-related fractures; external, related to ejecta patterns). To test for the presence of deep radial fractures on the moon, the azimuth and length of linear rim segments of twenty-four post-Imbrium-basin craters were measured. Linear segments of crater rims parallel preexisting fracture patterns in terrestrial craters floored in an indurated substrate. Craters forming in a terrain containing pervasive fractures radial to Imbrium should show evidence of this tectonic influence by forming rim crest segments (terrace scarps) preferentially along these directions. No systematic relation of these segments with Imbrium radial structure was found. This suggests that the surface radial grooves may not extend to depth. The relatively young Orientale basin shows two types of radial structures: (1) pervasive subparallel ridges and furrows formed by a spectrum of sizes of secondary crater chains emanating from the main crater, and from flowage of material during secondary cratering; (2) parallel, generally radial ridges which appear to have formed on top of outward flows of debris. These types of radial textures (both depositional and erosional) appear unrelated to major faults or fractures. Therefore, these two lines of evidence suggest that much of the Imbrium-type sculpture surrounding major lunar basins is sedimentary, rather than tectonic, in origin.

1. Introduction

Early telescopic studies of the Moon revealed a prominent surface texture composed of parallel ridges, grooves, and valleys. This distinctive texture was arranged in a pattern which was radial to the central portion of the Imbrium basin. Because of this distinctive association, the textured terrain came to be known as the 'Imbrium Sculpture" (Gilbert, 1893; see Hartmann, 1963, for extensive review of previous literature). This texture consists of two major components (Figure 1): (1) Broad linear valleys 3 to 12 km wide and up to 100–200 km in length and a series of smaller parallel ridges and grooves 1–4 km wide and tens of km in length. These latter features parallel the larger grooves but are more discontinuous in nature; (2) a series of extremely regular parallel ridges 1–2 km wide and tens of km long developed locally around the basin and distinct from the rougher textured linear components. These two components form the basic radial texture surrounding the Imbrium basin and their general characteristics and distribution have been described by Hartmann (1963). Similar radial textures have been documented around a number of other lunar basins including Orientale, Nectaris, Humorum, and Crisium (Hartmann, 1964). The origin of the texture, however, has been seriously debated since its first description. Theories of origin can be divided into two major groups (Figure 2): *Sedimentary theories* attribute the radial texture to erosional and depositional effects caused by material ejected from an impact crater which formed the Imbrium crater and basin (Gilbert, 1893; Baldwin, 1949, 1963; Urey, 1952). If the origin were wholly sedimentary, the texture should not extend to depth to any

The Moon **15** (1976) 445–462.

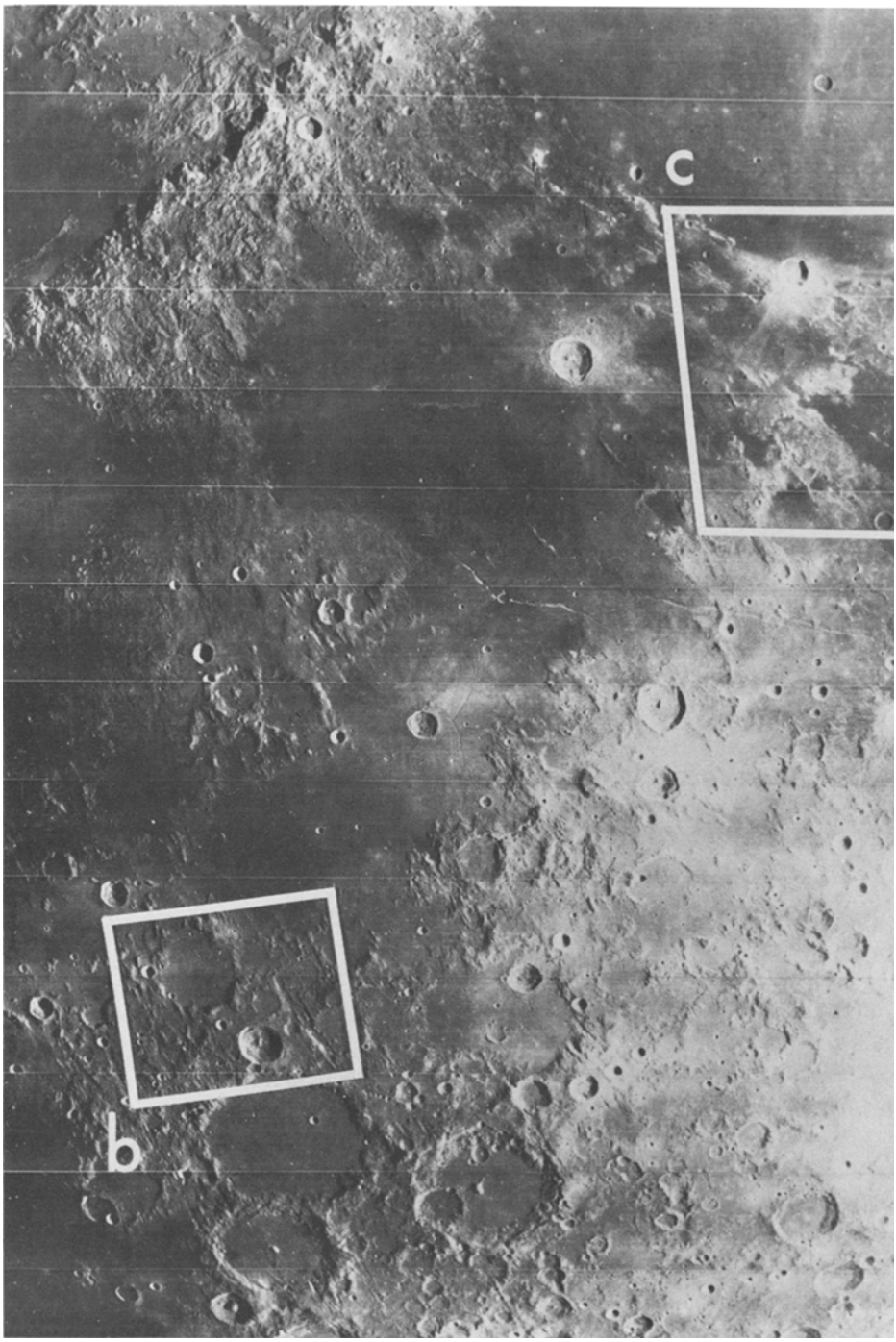

Fig. 1a. Distinctive radial texture southeast of the Imbrium basin (LO IV-102M).

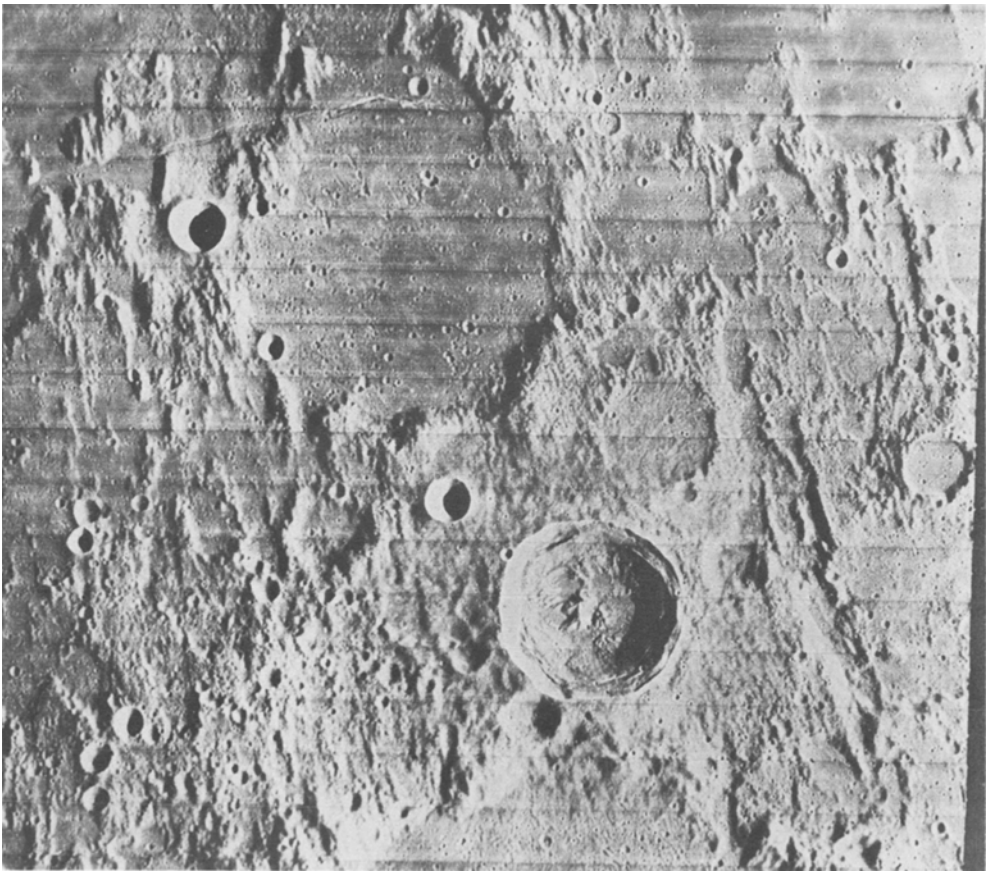

Fig. 1b. Broad linear valleys 3–12 km wide and over 100 km long; smaller parallel ridges and grooves 1–4 km wide and tens of km in length; large crater Flammarion in upper left is 75 km in diameter. Width of image is about 200 km. (LO IV-108H3).

appreciable degree. *Structural theories* attribute the radial texture to radial faults and fractures associated with the formation of the Imbrium basin (Spurr, 1945; Shoemaker, 1962; Hartmann, 1963, 1964; Strom, 1964; Scott, 1972; Scott *et al.*, 1975). In these theories, radial fractures propagate away from the basin interior causing visible lineations in the ground surface and downfaulting of major graben-like blocks radial to the basin. In this case, surface texture would be expected to extend to depth (Figure 2). Associated volcanic activity is often thought to be related to the postulated deep fractures (Scott, 1972).

In order to assess these possible theories of origin, a test was devised to gain information on the extent to which visible surface texture extends to depth. Impact craters undergo a modification stage in the terminal phases of the event, in which the walls of the crater slump into the crater interior, usually forming a series of linear terraces (Gault *et al.*, 1968). If the impact crater has formed in an area that contains regional lineaments or lines of structural weakness then the slumping tends to occur

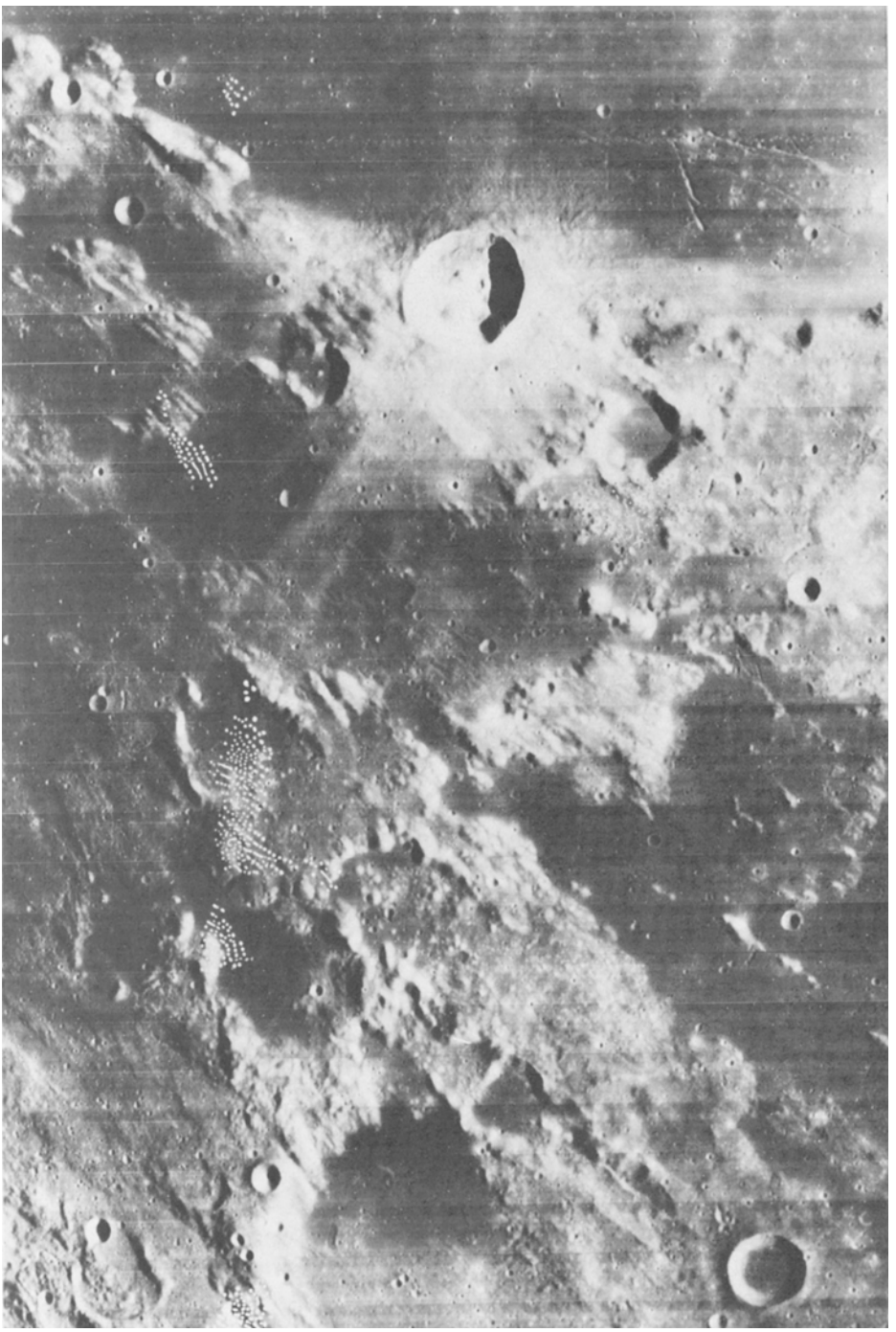

Fig. 1c. Region south of Serenitatis showing series of extremely regular parallel ridges 1–2 km wide and tens of km long developed radially to the Imbrium basin. Width of image is about 200 km. (LO IV-90H2).

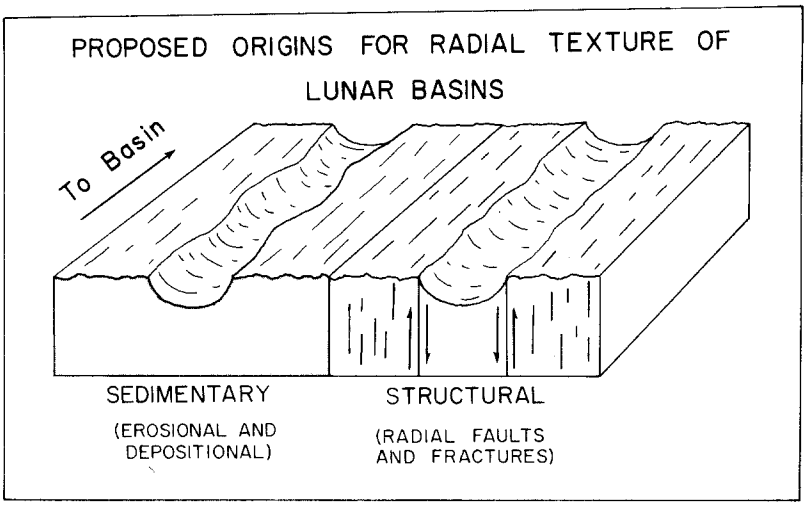

Fig. 2. Proposed origins for radial textures of lunar basins. Sedimentary texture (erosional and depositional) should not extend to depth, while texture formed structurally should extend to depth as near-vertical faults and fractures.

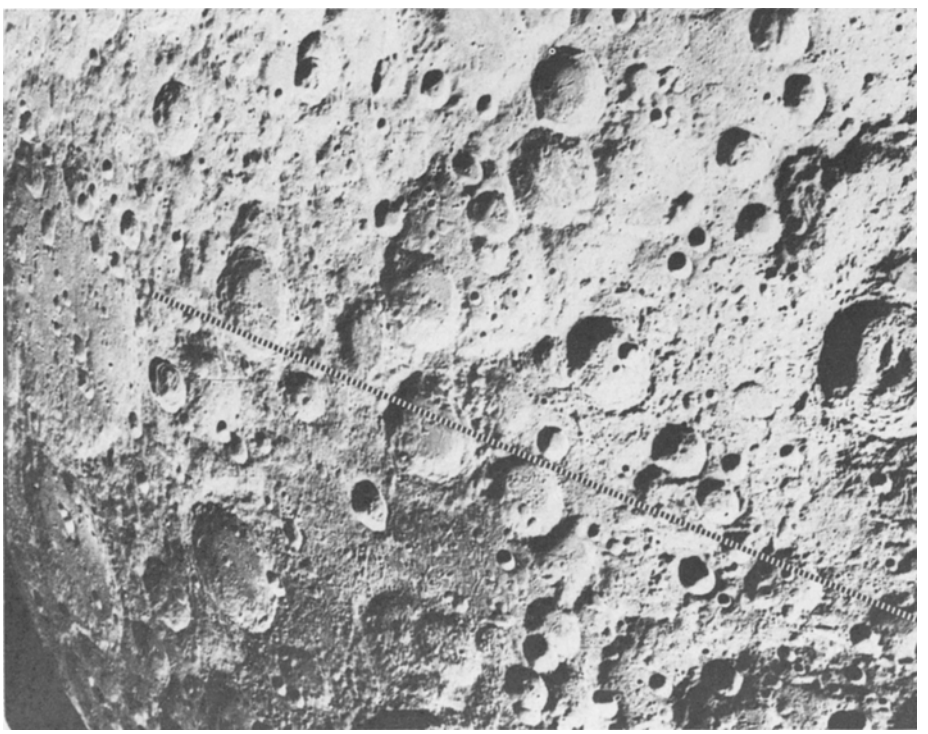

Fig. 3. Structural elements and crater rim crest alignment on the lunar far side.

Fig. 3a. Lineaments on farside unrelated to major basins in either orientation or morphology. Dashed line parallels major trends and is oriented approximately N55E. King crater (75 km) is seen in middle right.

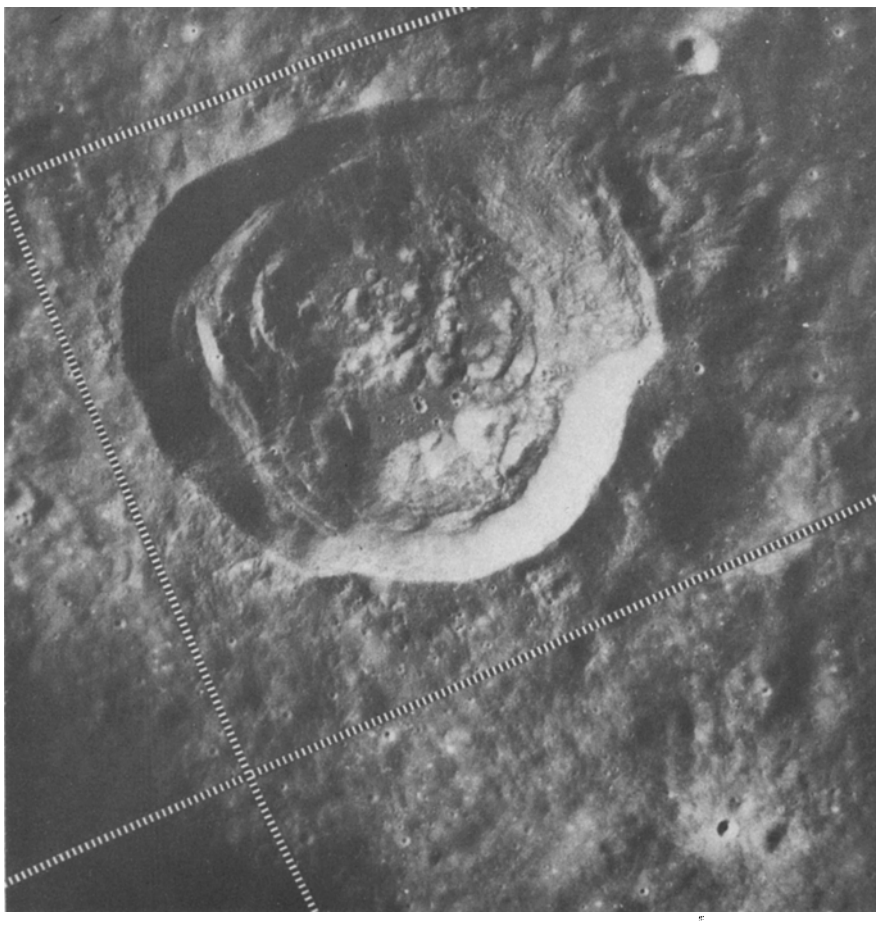

Fig. 3b. Rim crest segments aligned parallel and perpendicular to major lineament trend in 40 km crater (109°E, 09°S) located in left center of 3a.

preferentially along directions related to these lines of weakness as is seen in Meteor Crater, Arizona (Shoemaker, 1962, p. 310). Fulmer and Roberts (1963) have shown that the outline of the crater rim crest is dependent on the level of induration and the precratering fracture pattern of the target medium. However, where a layer of thick (relative to crater depth) unconsolidated material overlies rigid indurated material the crater outline is generally circular to subcircular. Therefore, only craters larger than 30 km, a size sufficient to have penetrated the surface fragmental layer (Head, 1976), were used in this study. For example, in an area of the lunar farside pictured in Figure 3a, a set of extensively developed parallel regional lineations can be seen which are not morphologically similar to basin radial texture and not radial to any basin. Numerous crater rim crests parallel these lineaments. Slumping of the walls occurs preferentially along and normal to the structural pattern as seen in the 40 km diameter crater in Figure 3b. This observation was then used to assess the extension to depth of the radial surface texture seen around the Imbrium basin.

2. The Imbrium Basin

The distribution of *major* elements of the radial surface texture surrounding the Imbrium basin is shown in Figure 4 and is summarized from Hartmann (1963). A number of areas are obscured by post-Imbrium mare deposits, particularly Serenitatis to the east and Oceanus Procellarum to the south and west. Twenty-four major post-Imbrium-basin craters were analyzed in this study (Figure 4). They ranged in size from 30 to 136 km in diameter and in age from Imbrian to Copernican (Table I). The location of craters examined ranged from the rim of the Imbrium crater, throughout the extensive surface texture, and out to about 1360 km from the center of the basin.

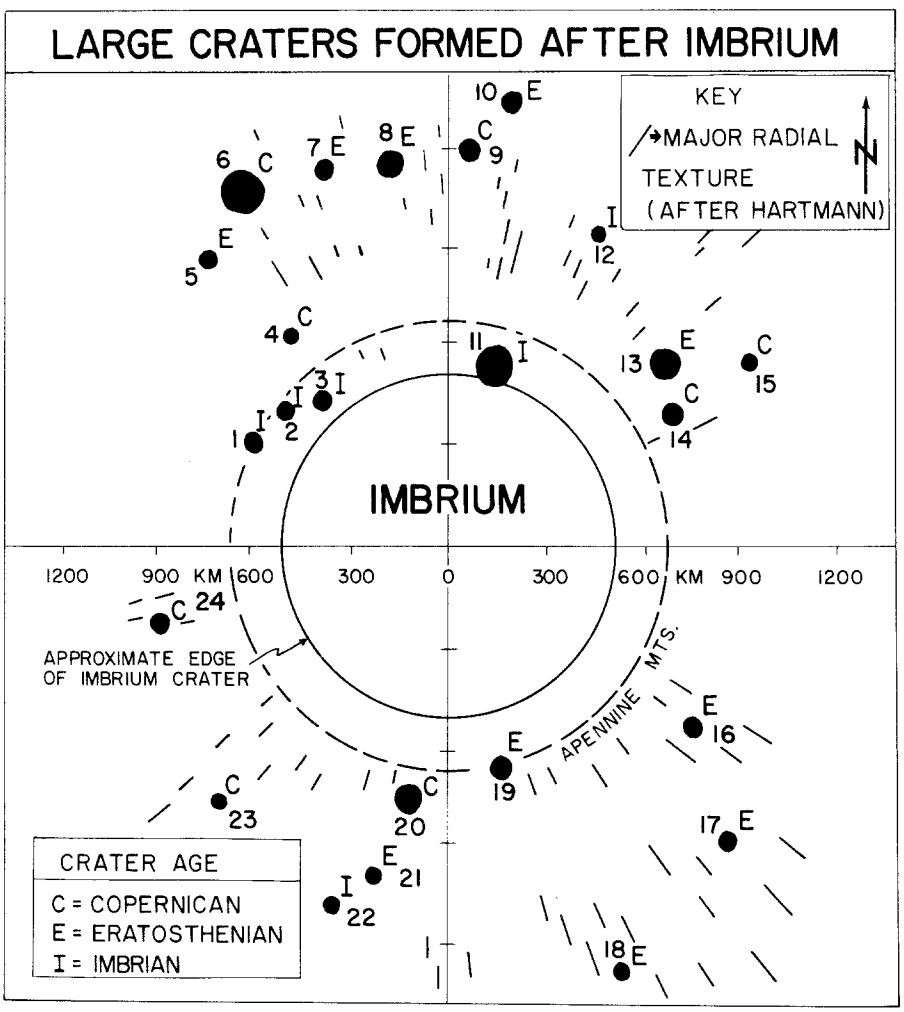

Fig. 4. Imbrium basin, illustrating major radial textural elements around Imbrium (after Hartmann, 1963). Also shown are the locations of 24 post-Imbrium age craters whose rim segments were measured. Crater numbers are keyed to Table I.

TABLE I

Crater name	Diameter (km)	Location	Distance from center of Imbrium (km)	Direction from center of Imbrium	Age (C = Copernican) (E = Eratosthenian) (I = Imbrium)	Target material (H = Highlands) (M = Mare)	Number of rim crest segments measured	Major trend	Minor trends
1. Mairan	40	42°N 44°W	650	N64°W	Ic_2	H	15	N85°W	N25°E
2. Sharp	41	46°N 40°W	600	N51°W	Ic_2	H	15	N25°W	N5°E, N85°E
3. Bianchini	39	48°N 35°W	550	N42°W	Ic_2	H	15	N35°E	N55°W, N35°W N65°E, N15°W
4. Harpalus	40	53°N 43°W	760	N38°W	Cc_1	M	16	N25°E	N25°W
5. Markov	40	53°N 63°W	1100	N46°W	Ec	H M	16	N35°E	N75°E, N5°E
6. Pythagoras	136	64°N 63°W	1240	N31°W	Cc_1	H	27	N85°W	N25°W, N25°E, N5°E
7. Carpenter	63	69°N 52°W	1150	N19°W	Ec	H	14	N5°W	N85°E, N65°E
8. Philolaus	75	72°N 34°W	1160	N 9°W	Ec	H	15	N55°E	N85°W, N15°W, N85°E, N25°E
9. Anaxagoras	52	74°N 10°W	1170	N 3°E	Cc	H	16	N35°E	N85°W
10. Scoresby	57	78°N 13°E	1330	N 8°E	Ec	H	15	N55°E	N15°W
11. Plato	106	52°N 9°W	510	N14°E	Ic_2	H	26	N75°E	N35°E, N85°E
12. C. Mayer	41	63°N 17°E	1030	N 3°E	Ic_2	H M	13	N85°W	N35°W
13. Aristoteles	90	50°N 17°E	860	N48°E	Ec	H M	22	N35°W	N55°E, N85°E
14. Eudoxus	70	44°N 16°E	790	N60°E	Cc_1	H M	12	N5°W	N75°E, N35°E
15. Burg	39	45°N 28°E	1050	N59°E	Cc_1	M	12	N35°E	N45°W, N65°E, N35°W
16. Manilius	38	15°N 9°E	940	S55°E	Ec	H	14	N55°W	N45°E
17. Agrippa	45	4°N 11°E	1230	S45°E	Ec	H	18	N75°W	N65°E, N35°W
18. Herschel	40	6°S 2°W	1380	S25°E	E	H	13	N75°E	N45°W
19. Eratosthenes	60	15°N 11°W	650	S14°E	Ec	H	30	N45°W	N15°E, N85°E
20. Copernicus	95	10°N 20°W	800	S 9°W	Cc_1	H	37	N65°W	N45°E
21. Reinhold	45	3°N 23°W	1010	S13°W	Ec	H	20	N5°E	N55°E, N45°W
22. Lansberg	38	1°527°W	1150	S18°W	Ic_2	M	16	N35°W	N45°E, N85°E, N15°W, N15°E
23. Kepler	32	8°N 38°W	1020	S42°W	Cc_2	H	13	N85°E	N25°W
24. Aristarchus	41	23°N 48°W	890	S75°W	Cc_2	H	14	N65°W	N35°W

Linear segments of crater rim crests for each of the twenty-four craters were measured and plotted on azimuth-frequency diagrams. Major, and significant minor peaks for each crater (Table I) are summarized in Figure 5. If the basin radial texture extended to depth, one would expect many of the rim crest segment peaks to be radial and perhaps normal to the basin. Instead they appear generally randomly distributed (Figure 5). In addition, there appears to be no significant correlation of major peaks with size or age of crater. The lack of significant crater rim crest alignment related to the Imbrium radial texture strongly suggests that the texture does not extend to depth and is therefore not structural in origin. There is some suggestion of preferential alignment of major trends in northwest and northeast directions, two major directions of lunar grid patterns (Strom, 1964).

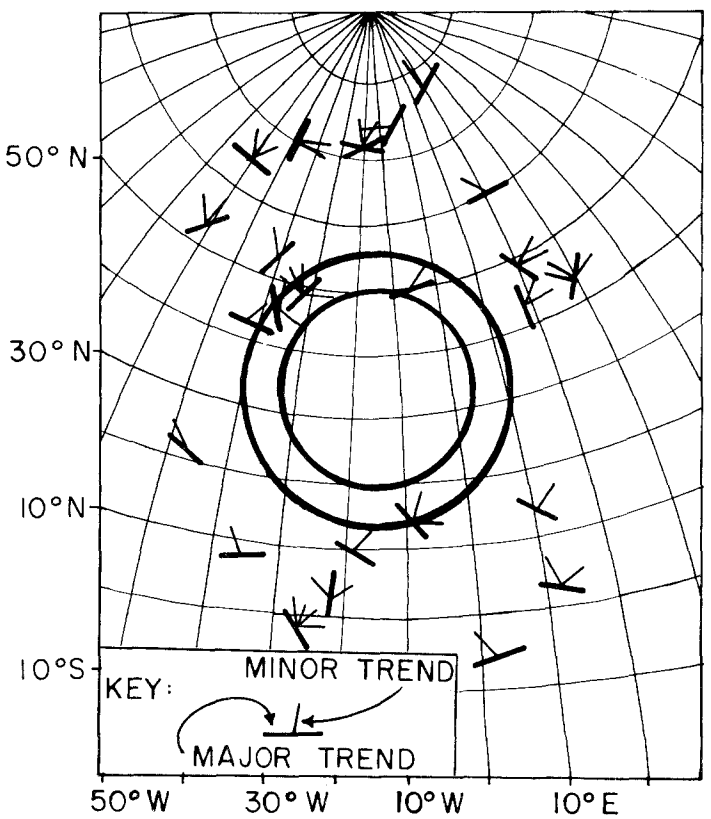

Fig. 5. Trends of crater rim crest segments of 24 post-Imbrium age craters plotted on a stereographic base with the center of Imbrium at the center of the disc. Solid lines represent the major trends. Smaller lines represent minor trends. Grid is 10°; center of Imbrium approximately 35°N 16°W. Outer ring is the Apennine ring.

3. The Orientale Basin

Additional evidence concerning the origin of basin radial texture was provided when Lunar Orbiter photography revealed the details of a large basin on the western limb of the Moon. The Orientale basin, some 900 km in diameter, is younger than

Imbrium and the youngest and most well preserved of the lunar basins (McCauley, 1968). Extensive radial texture surrounds the Orientale basin (Hartmann, 1964; Head, 1973; Howard *et al.*, 1974; Moore *et al.*, 1974) and its relatively well-preserved nature provides evidence for origin of the texture.

One of the major components of radial texture associated with the Orientale basin is a series of valleys which extend from the basin edge outward. These valleys are similar to the major troughs surrounding the Imbrium basin and average 5 to 20 km wide and several hundred kilometers long. These troughs are made up of distinct series of intersecting craters and can be seen to lead outward into discontinuous chains and clusters of secondary craters (Figure 6). This type of morphology is characteristic of chains of craters formed by impact of strings and filaments of ejecta from large craters (Morrison and Oberbeck, 1975). None of the major troughs surrounding Orientale differs markedly from this characteristic crater

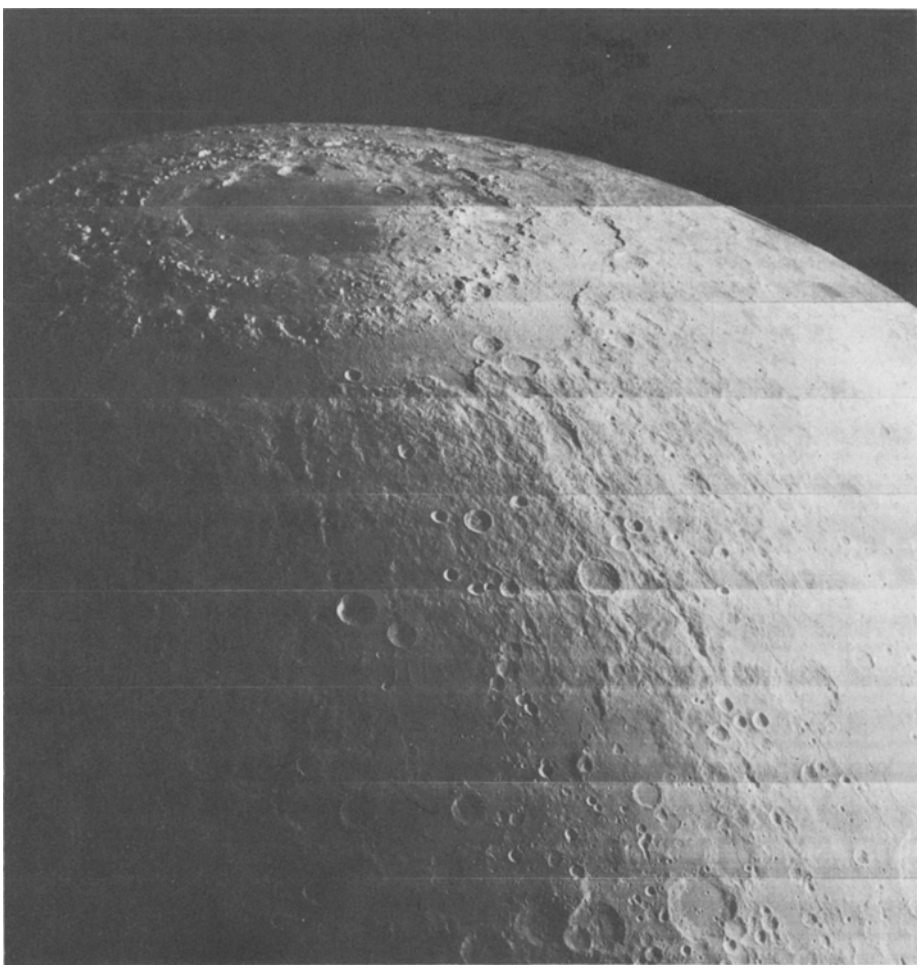

Fig. 6. Major troughs leading radially away from the Orientale basin. Troughs average 5–20 km wide and are up to hundreds of km in length. View looking NNW over Orientale (LO IV-193M).

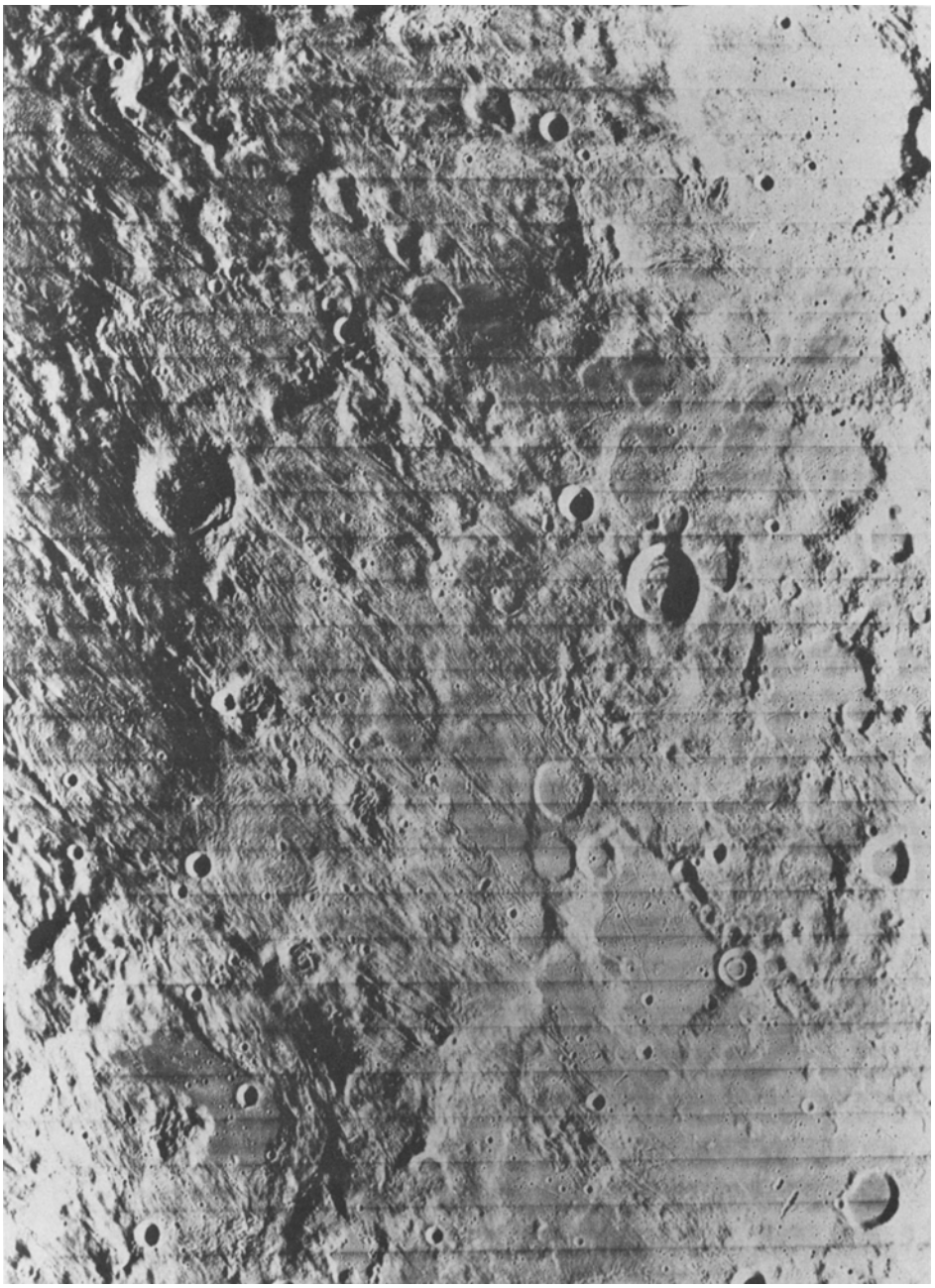

Fig. 7. Finely grooved and furrowed terrain southeast of the Orientale basin. The texture is generally radial but deviates where it encounters steep slopes, such as along northeast wall of large crater in lower left of photograph. Width of image is about 285 km. (LO IV-167H3).

Fig. 8a. Sherman landslide, Alaska. a. Viewed from west. Debris fell from peak at right, and crossed the 2.5 km wide Sherman Glacier. Thickness of debris 3–6 m; volume $3 \times 10^7 M^3$.

chain morphology. The fresher Orientale radial valleys preserve the crater-chain aspect of these features. Since these features are demonstrably erosional rather than structural, this strongly suggests that the analogous, but less well-preserved portion of Imbrium basin radial texture has an erosional sedimentary origin.

Additional types of radial texture can be seen surrounding Orientale, which are analogous to other radial components surrounding Imbrium. In particular a finely grooved and furrowed radially textured terrain can be mapped in the region several hundred kilometers from the basin rim (Figure 7). In detail the region consists of distinctly parallel sets of grooves, ridges and furrows and is similar to one component of Imbrium radial texture in dimensions and location relative to the basin. The texture is radial in flat to hummocky terrain. However, it deviates from this parallelism when slopes begin to steepen, such as along pre-existing crater walls (Figure 7). Other examples of this type of behavior are prominent around the Orientale basin and occasionally radial texture merges with concentric texture (Figure 7). In a homogeneous crust, vertical radial fractures should tend to pass through local topographic variations without substantial deviations. Therefore, the deviations seen in these radial textures may be associated with surface movement of materials rather than deep radial structure. An additional example of this can be

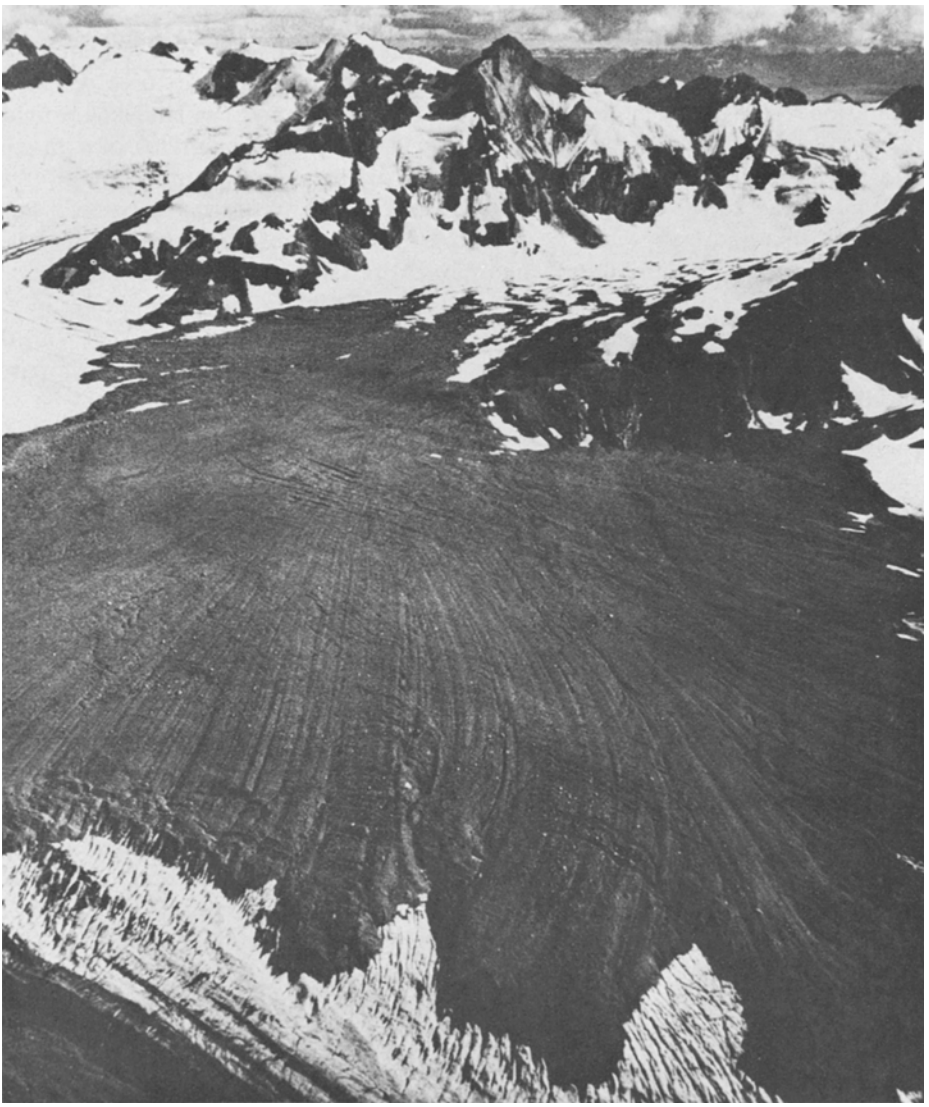

Fig. 8b. Surface and distal edge of landslide looking toward landslide source. Lobe width (center foreground) about 300 m. Note longitudinal grooves and variation in groove orientation with local direction of movement. Compare to lower left of Fig. 8a. Photographs by Austin Post, U. S. G. S. From Shreve (1966).

seen in the nearby crater Inghirami. Studies of the ejecta surrounding Orientale indicate that some portions of the outer ejecta blanket behaved like a landslide in the latest stages of ejecta deposition (Head, 1973). Terrestrial landslides show interesting comparisons. The Sherman Glacier landslide (Figure 8) extends for a distance of 6 km from its point of origin out over the Sherman Glacier. The landslide surface displays a distinctive series of parallel grooves and ridges which are essentially parallel to the direction of flow. In the Sherman and other slides,

these are interpreted as planes of shear developed where one portion of the landslide is moving at a slightly different rate than an adjacent part (Heim, 1882; Shreve, 1966; Hsu, 1975). It is important to note that these textures deviate in orientation where flow lobes have followed local topography. The landslide provides an example of how this type of texture can develop on the surface of a moving mass of debris. Based on the characteristics of their surface morphology, their position relative to the basin, and their textural similarity to some terrestrial landslides, this textured component is interpreted to be depositional and sedimentary in origin, rather than representing a surface expression of deep radial fractures. In summary, radial textures of a variety of types surrounding the Orientale basin can be attributed to several modes of ejecta erosion and deposition associated with the formation of the Orientale impact crater (Head, 1973; Moore *et al.*, 1974; Morrison and Oberbeck, 1975).

4. Discussion

From the evidence cited above, the radial texture surrounding the Imbrium and Orientale basins is believed to be sedimentary, rather than tectonic in origin. Since considerable seismic energy must have been expended during the formation of these large basins (Titley, 1966; Schultz and Gault, 1975) it is important to consider how effects from this seismic energy might be manifested.

4.1. Location of deformation zone

The majority of major visible structural deformation associated with impact craters is apparently concentrated within about a crater diameter from the center of the crater. The most intense deformation is usually associated with the vertical uplift of the inner portion of the crater rim. The vast majority of linear textures discussed here lie at distances greater than two crater radii from the center of the basins. For many of the basins, there is abundant evidence of structural deformation within two crater radii. The scarps which define the basins themselves (Cordillera Mountains-Orientale basin; Apennines, Caucasus-Imbrium basin) are believed to be concentric ring faults which formed when large portions of the basin rim collapsed inward toward the newly-formed crater (Head, 1974b; Howard *et al.*, 1974). Large, isolated valleys radial to the basin are often developed at the crater rim or between the crater rim and the ring fault (Alpine Valley-Imbrium basin; Taurus-Littrow Valley-Serenitatis basin; unnamed examples in the Orientale basin). These have been interpreted as large graben forming close to the crater rim in the most intense zone of deformation (Head, 1974a, b). The distribution of these structures around basins and the orientation of major elements of the basin ring faults appear to be related to pre-existing NW and NE structural grains. Thus, major visible structural elements are concentrated near the crater rim, and their distribution appears to be influenced by pre-existing structural trends.

4.2 Propagation of radial structural dislocations

In small-scale hypervelocity impacts into solid rock targets, extent of propagation of radial fractures is related to the homogeneity and density of the material, with greatest extent seen in homogeneous materials of low porosity (Moore *et al.*, 1961;

Hörz, 1969). Larger terrestrial craters, such as natural impacts and nuclear explosions have associated fracture patterns that are closely related to preexisting inhomogeneities in the target material. Underground nuclear explosions produce fractures in alluvium which are dominantly related to pre-existing joint patterns in underlying bedrock (Barosh, 1968). In the case illustrated in Fig. 9, radial fractures lie predominantly within two crater radii (collapse crater), but their distribution is strongly controlled by regional fracture trends (generally NE in this region). All additional fractures show an even closer relation to the pre-existing NE joint trend (Barosh, 1968). Radial fractures in Canadian craters (from which overlying ejecta deposits have largely been stripped) are not abundant, are confined to the vicinity of the crater, and quickly merge with regional structural patterns (Dence *et al.*,

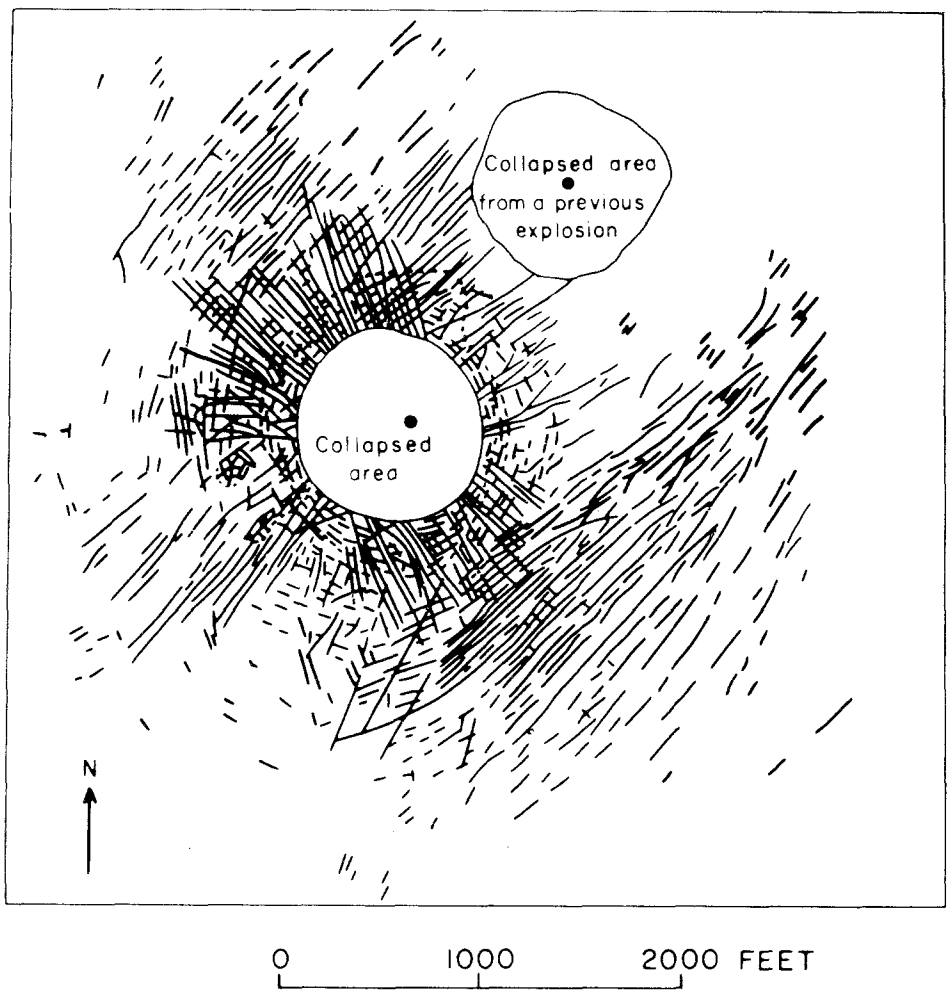

Fig. 9. Fractures produced above an underground nuclear explosion, Yucca Flat, Nevada (from Barosh, 1968; mapped by T. L. Prather). Most radial fracturing is confined to the vicinity of the crater. The majority of fractures represent movement along old fracture trends.

1968; Currie, 1971; 1972). It appears, then, that most materials are compositionally and structurally inhomogeneous at the scale of large cratering events and that radial fractures therefore do not propagate far from the crater rim.

4.3. Fault dislocation related to cratering events

Detailed work with nuclear explosions has shown that these events modify the existing strain field by triggering motion along planes of weakness (Press and Archambeau, 1962; Toksoz *et al.*, 1964; Smith *et al.*, 1969). In many cases, associated seismic activity and fault movement result in large part from explosion-initiated release of natural tectonic strain (Hamilton *et al.*, 1969). Since levels of natural tectonic strain in the lunar crust are less than in the Earth's crust (Latham *et al.*, 1973) (as they probably were even in late pre-Imbrian time), fault dislocations in analogous lunar events may not show as extensive dislocations as those seen in terrestrial events.

4.4. Timing of sedimentary and seismic events

Based on speed of travel of seismic waves and material ejected from lunar basins (Schultz and Gault, 1975; Oberbeck *et al.*, 1973) the vast majority of potential radial dislocation should have taken place prior to the deposition of ejecta. Thus, even if radial fractures had propagated large distances from the basin, they would probably have been heavily eroded by the rapidly following arrival of the ejecta. The visible texture would therefore be dominated by the sedimentary aspects of ejecta deposition. Evidence for radial fractures should then be visible in post-event crater terraces.

In summary, major radial structural dislocations are confined to the region of the crater rim, and radially dispersed seismic energy is largely absorbed by pre-existing structural inhomogeneities rather than in the creation of a widespread set of radial fractures. Any structural dislocations which do form away from the basin rim area may largely be obliterated by the arrival and deposition of basin ejecta.

5. Conclusions

In conclusion, an analysis of the orientation of rim crest segments for 24 post-Imbrium craters strongly suggests that the radial texture surrounding the Imbrium basin does not extend to depth and is therefore surficial in nature. Orientation of rim crest segments shows some correlation with previously described pre-Imbrium basin structural grid patterns. Radially propagating seismic energy associated with the Imbrium cratering event may have been preferentially absorbed along these pre-existing trends, rather than forming extensive surface radial features and troughs. Examination of the characteristic radial texture of the younger Orientale basin indicates that the Orientale radial texture is associated with several modes of basin ejecta erosion and deposition and is therefore essentially a surficial feature. The radial texture surrounding the older Imbrium basin appears to be a slightly more degraded version of the main components of the Orientale radial texture. It is concluded that the extensive Imbrium radial texture is surficial and sedimentary in nature, being associated with ejecta deposits of the basin event.

Acknowledgements

This work was performed under National Aeronautics and Space Administration grant NGR-40-002-116, which is gratefully acknowledged. Thanks are extended to the National Space Science Data Center for providing many of the photographs used in this study. Mr Bruce Wilks provided extensive help in the plotting and numerical analysis of crater rim crest segments. Helpful criticisms and reviews were provided by M. Cintala, R. D'Alli, B. R. Hawke, R. Jennings, and M. Settle.

References

Baldwin, R. B.: 1949, *The Face of the Moon*, Chicago, University of Chicago Press.

Baldwin, R. B.: 1963, *The Measure of the Moon*, Chicago: University of Chicago Press.

Barosh, P. J.: 1968, 'Relationships of Explosion-produced Fracture Patterns to Geologic Structure in Yucca Flat, Nevada Test Site', *Geol. Soc. Am. Mem.* **110**, 199–217.

Currie, K. L.: 1971, 'Geology of the Resurgent Cryptoexplosion Crater, at Mistastin Lake, Labrador', *Geological Society of Canada, Bull.* **207**, 62 p.

Currie, K. L.: 1972, 'Geology and Petrology of the Manicouagan Resurgent Caldera, Quebec', *Geological Survey of Canada, Bull.* **198**, 153 p.

Dence, M. R., Innes, M. J. S., and Robertson, P. B.: 1968, 'Recent Geological and Geophysical Studies of Canadian Craters', In *Shock Metamorphism of Natural Materials* (Bevan M. French and Nicholas Short, eds.), Mono Book Corp., Baltimore, pp. 339–362.

Fulmer, C. and Roberts, W.: 1963, 'Rock Induration and Crater Shape', *Icarus* **2**, 452–465.

Gault, Donald E., Quaide, W. L., and Oberbeck, V. R.: 1968, 'Impact Cratering Mechanics and Structures', In *Shock Metamorphism of Natural Materials* (Bevan M. French and Nicholas M. Short, eds.), Mono Book Corp., Baltimore, pp. 87–99.

Gilbert, G. K.: 1893, *Bull. Phil. Soc. Wash.* **12**, 241.

Hamilton, R. M., McKeown, F. A., and Healy, J. H.: 1969, 'Seismic Activity and Faulting Associated with a Large Underground Nuclear Explosion', *Science* **166**, 601–604.

Hartmann, W. K.: 1963, 'Radial Structures Surrounding Lunar Basins, I: The Imbrium Systems', *Commun. Lunar Planet. Lab.* **2**, 1–15.

Hartmann, W. K.: 1964, 'Radial Structures Surrounding Lunar Basins, II: Orientale and Other Systems; Conclusions', *Commun. Lunar Planet. Lab.* **2**, 175–191.

Head, J. W.: 1973, 'Origin of Morphologic Components of the Hevelius Formation: Lunar Orientale Basin (abs.)', *GSA Annual Meetings, Abstract with Programs*, 1973, pp. 661.

Head, J. W.: 1974a, 'Morphology and Structure of the Taurus-Littrow Highlands (Apollo 17): Evidence for their Origin and Evolution', *The Moon* **9**, 355–395.

Head, J. W.: 1974b, 'Orientale Multi-ringed Basin Interior and Implications for the Petrogenesis of Lunar Highland Samples', *The Moon* **11**, 327–356.

Head, J. W.: 1975, 'Processes of Lunar Crater Degradation: Changes in Style with Geologic Time', *The Moon* **12**, 299–329.

Head, J. W.: 1976, 'The Significance of Substrate Characteristics in Determining Morphology and Morphometry of Lunar Craters'. *Lunar Science VII*, Lunar Science Institute, pp. 354–356.

Heim, A.: 1882, 'Der Bergsturz von Elm', *Deutsch. Geol. Gesell. Zeitschr.* **34**, 74–115.

Hörz, F.: 1969, 'Structural and Mineralogical Evaluation of an Experimentally Produced Impact Crater in Granite', *Contr. Mineral. and Petrol.* **21**, 365–377.

Howard, K. A., Wilhelms, D. E., and Scott, D. H.: 1974, 'Lunar Basin Formation and Highland Stratigraphy', *Rev. Geophys. Space Phys.* **12**, 309–327.

Hsu, K. J.: 1975, 'Catastrophic Debris Streams (Sturzstroms) Generated by Rockfalls', *GSA Bull.* **86**, 129–140.

Latham, G., Dorman, J., Duennebier, F., Ewing, M., Lammlein, D., and Nakamura, Y.: 1973, 'Moonquakes, Meteoroids, and the State of the Lunar Interior', *Proc. Lunar Sci. Conf. 4th*, **3**, 2515–2527.

McCauley, J. F.: 1968, 'Geologic Results from the Lunar Precursor Probes', *Am. Inst. Aeronautics and Astronautics J.* **6**, 1991–1996.

Moore, H. J., Gault, D. E., and Lugn, R. V.: 1961, 'Experimental Hypervelocity Impact Craters in Rock'. *Proc. Fifth Hypervelocity Impact Symposium*, Denver, Co., **1**, 625–643.

Moore, H. J., Hodges, C. A., and Scott, D. H.: 1974, 'Multi-ringed Basins – Illustrated by Orientale and Associated Features', *Proc. Fifth Lunar Sci. Conf.* **1**, 71–100.

Morrison, R. H. and Oberbeck, V. R.: 1975, 'Geomorphology of Crater and Basin Deposits – Emplacement of the Fra Mauro Formation', *Proc. Lunar Sci. Conf. 6th*, p. 2503–2530.
Oberbeck, V. R., Hörz, F., Morrison, R. H., and Quaide, W. L.: 1973, Emplacement of the Cayley Formation', *NASA Technical Memorandum*, X-62, 302.
Press, F. and Archambeau, C.: 1962, *J. Geophys. Res.* **67**, 337.
Schultz, P. H. and Gault, D. E.: 1974, 'Seismic Effects from Major Basin Formation on the Moon and Mercury', *The Moon* **12**, 159–177.
Scott, D. H.: 1972, 'Structural Aspects of Imbrium Structure', *Apollo 16 Preliminary Science Report*, Sec. 29, pp. 31–33.
Scott, D. H., Diaz, J. M., and Watkins, J. A.: 1975, 'The Geologic Evaluation and Regional Synthesis of Metric and Panoramic Photographs', *Proc. Lunar Sci. Conf. 6th*, p. 2531–2540.
Shoemaker, E. M.: 1962, *Physics and Astronomy of the Moon* (Z. Kopal, ed.), chapt. 8, New York: Academic Press, Inc.
Shreve, R. L.: 1966, 'Sherman Landslide, Alaska', *Science* **154**, 1639–1643.
Smith, S. W., McGinley, Jr., J., Scholz, C., and Johnson, L.: 1969, 'Effects of Large Explosions on Tectonic Strain', *J. Geophys. Res.* **74**, 3308–3309.
Spurr, J. E.: 1945, *Geology Applied to Selenology*, V. 1, Lancaster, Pa.: Science Press.
Strom, R. G.: 1964, 'Analysis of Lunar Lineaments, I: Tectonic Maps of the Moon', *Commun. Lunar Planet. Lab.* **2**, pp. 205–216.
Titley, S. R.: 1966, 'Seismic Energy as an Agent of Morphologic Modification on the Moon', Astrogeologic Studies Annual Prog. Rept., December 1966, U. S. G. S., Open File Report, pp. 87–104.
Toksöz, M. N., Ben-Menaham, A., and Harkrider, D. G.: 1965, *J. Geophys. Res.*, V. 70, pp. 907
Urey, H. C.: 1952, *The Planets, Their Origin and Development*, New Haven: Yale University Press.